Journal of Modern Optics

ISSN: 0950-0340 (Print) 1362-3044 (Online) Journal homepage: https://www.tandfonline.com/loi/tmop20

An evanescent field absorption gas sensor at mid-IR 3.39 μm wavelength

M. A. Butt, S. A. Degtyarev, S. N. Khonina & N. L. Kazanskiy

To cite this article: M. A. Butt, S. A. Degtyarev, S. N. Khonina & N. L. Kazanskiy (2017) An evanescent field absorption gas sensor at mid-IR 3.39 μm wavelength, Journal of Modern Optics, 64:18, 1892-1897, DOI: 10.1080/09500340.2017.1325947

To link to this article: https://doi.org/10.1080/09500340.2017.1325947

Published online: 09 May 2017.

JOURNAL OF MODERN OPTICS, 2017
VOL. 64, NO. 18, 1892–1897
https://doi.org/10.1080/09500340.2017.1325947

Taylor & Francis
Taylor & Francis Group

An evanescent field absorption gas sensor at mid-IR 3.39 μm wavelength

M. A. Butt[a], S. A. Degtyarev[a], S. N. Khonina[a,b] and N. L. Kazanskiy[a,b]

[a]Samara National Research University, Samara, Russia; [b]IPSI RAS – Branch of the FSRC "Crystallography and Photonics" RAS, Samara, Russia

ABSTRACT

Trace gases such as H_2O, CO, CO_2, NO, N_2O, NO_2 and CH_4 strongly absorb in the mid-IR (>2.5 μm) spectral region due to their fundamental rotational and vibrational transitions. CH_4 gas is relatively non-toxic, however, it is extremely explosive when mixed with other chemicals in levels as low as 5% and it can cause death by asphyxiation. In this work, we propose a silicon strip waveguide at 3.39 μm for CH_4 gas sensing based on the evanescent field absorption. These waveguides can provide the highest evanescent field ratio (EFR)>55% with adequate dimensions. Moreover, EFR and sensitivity of the sensor are highly dependent on the length of the waveguide up to a certain limit. Therefore, it is always a compromise between the length of the waveguide and EFR in order to obtain greater sensitivity.

ARTICLE HISTORY
Received 17 April 2017
Accepted 23 April 2017

KEYWORDS
Strip waveguide; methane gas; evanescent field ratio; mid-IR

Introduction

Chemical sensing is one of the emerging and important applications for integrated photonics outside of telecommunications. Absorptive or luminescent properties of a medium/ layer located in the evanescent wave region of the propagating mode are measured. Gas sensors are widely used in various fields such as chemistry, biology, medicine, manufacturing and environmental industry (*1*). Mainly gas sensors comprise catalytic, electrochemical, thermal, ultrasonic, semiconductor and infrared sensors. Their detection mechanisms can depend on the thermal, chemical, mechanical, electrical or optical property of the functional materials (*2*). Nevertheless, most of these sensors are massive and some even need a thermal management system (*2*). Their compactness and manageability are limited; therefore they are not applicable in the circumstances where inadequate space is available. It is attractive to have miniature sensors that could be tailored to small chip areas. In this way, they could be integrated with on-chip control and processing circuits to build chip-scale sensing systems, which can be deployed in distributed sensing networks.

Various approaches have been employed in the design and fabrication of fibre-optic chemical sensors. The most widespread approaches are absorption-based or fluorescence-based systems. Direct absorption sensors depend on the measure and retaining characteristic absorption lines. Therefore, the concentration of the species can be directly related to the optical attenuation at a specific wavelength. Different gases and their concentration affect the absorption experienced by the evanescent field. This exploited the realization of gas sensors as has been shown in fibre optics (*3–5*). Moreover, the fibre optics and waveguide technology are well-developed and established in the near-IR telecommunication band. There are very few types of industrially or environmentally important gases with absorption peaks in the near-IR wavelengths. However, mid-IR spectrum window contains absorption peaks for an extensive variety of trace gases, including H_2O, CO, CO_2, NO, N_2O, NO_2 and CH_4 (*3, 6*). If sustainable, wavelength-based sensors for these gases are available at affordable price, they can be integrated with electrical circuitry to support system on-chip applications for industrial and environmental monitoring. For instance, methane (CH_4) has weak absorption lines at 1.33 and 1.66 μm and its strong fundamental absorption at 3.3 μm. The wavelength region between 3 and 3.7 μm is principally significant because it contains essentially all the characteristic stretching frequencies of the molecules containing C–H bonds. The strength of the fundamental absorptions in this so-called C–H stretch region can be orders of magnitude higher than overtone absorptions of the same molecules in the near-infrared (NIR). For example, the absorption of CH_4 at 3.3 μm is 100 times stronger than in its overtone band at 1.65 μm. The optical fibre or

CONTACT M. A. Butt muhammadali.butt1985@gmail.com

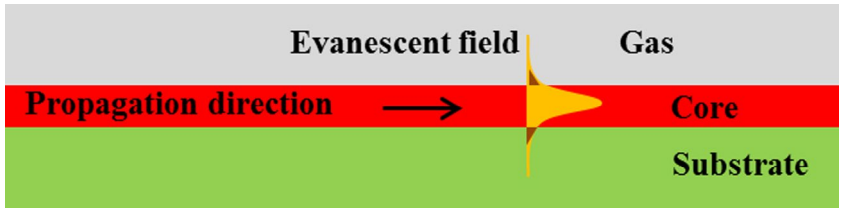

Figure 1. Schematic of the evanescent absorption gas sensor.

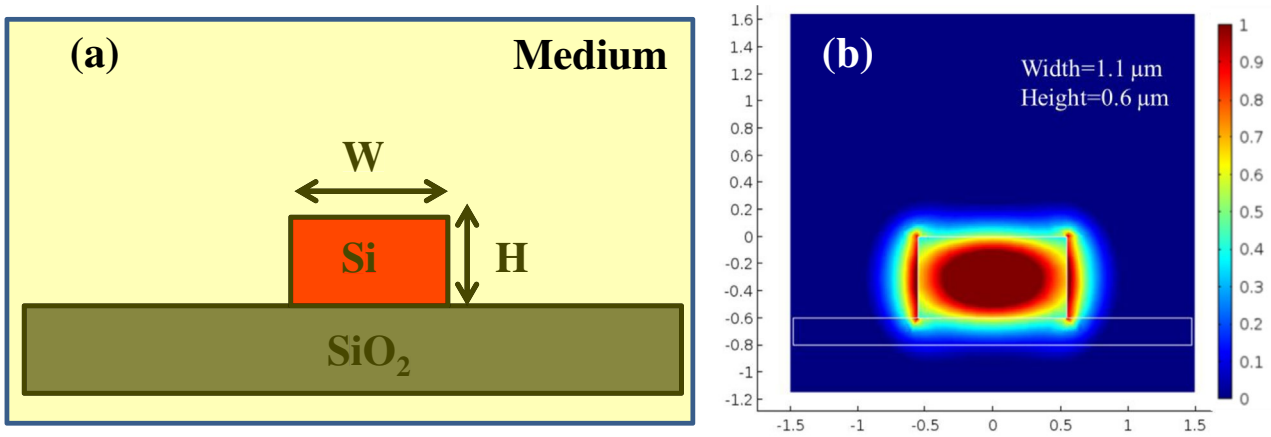

Figure 2. (a) Schematic of a strip waveguide and (b) quasi-TE mode distribution in a strip waveguide at 3.39 microns (W = 1.1 microns, H = 0.6 microns).

waveguide has three main purposes. In the simplest case, the fibre is only used to transfer the light to and from a spectroscopic cell and shows no direct involvement in the sensing (*7–9*). In the second methodology, indicator dyes are immobilized at the fibre tip. Last but not the least, the fibre or waveguide itself forms the sensing element using the evanescent field extending from the core to interact with the chemical species (*10, 11*). This method is of particular interest as it allows the development of distributed sensor systems.

Methane gas comes from the earth as well as from our bodies. CH_4 is relatively non-toxic as it doesn't have an OSHA PEL standard (*12*). Moreover, it can be harnessed as an energy source. However, it is extremely explosive and it can cause death by asphyxiation (*13*). It is important to apprehend the hazards related to the methane gas. It can become explosive when mixed with other chemicals in levels as low as 5%. When mixed with hydrogen sulphide, it gives a smell like rotten egg and can be easily detected. In places where an unpleasant rotten egg smell is noticed, the CH_4 levels may be high enough to become explosive. Under high concentrations, CH_4 gas can be deadly when ignited. Natural CH_4 gas from beneath the earth has caused disastrous mining and oil rig explosions. Although it is non-toxic, but it is a simple asphyxiant because it can displace oxygen from the body which is desirable for breathing. Oxygen levels below 16% can be dangerous and levels below 10% can be deadly. There is no specific standard governing the permitted amount of CH_4 in the air at home/ workplace, but the minimum oxygen content for any place where people need to breathe is 18%. CH_4 gas on its own isn't deadly; it has the potential to turn into poisonous when mixed with other substances. The burning of natural gas (97% CH_4) without any proper air circulation can produce carbon monoxide. Carbon monoxide is a deadly gas because it is difficult to detect. Relatively low levels of carbon monoxide can cause dizziness and nausea within 20 min and death within two hours. Higher levels can kill within three minutes. The centres for disease control and prevention estimates that carbon monoxide poisoning kills 500 people each year. In this paper, we propose evanescent field absorption CH_4 gas sensor based on strip waveguide in mid-IR absorption wavelength. When the electromagnetic wave travels through the silicon strip waveguide, most of the energy is confined within the core. However, there is a part of light known as evanescent field extending to the substrate and cladding region as shown in Figure 1.

In the cladding region, the wave interacts with the gas surrounding the waveguide. The light goes through power attenuation if the wavelength is properly selected with the absorption lines of the CH_4 gas. The absorption is widely dependent on the concentration of the gas under consideration. Therefore, evanescent field ratio (EFR) is an important parameter for the realization of gas sensors based on the absorption of the evanescent field. The EFR

is the ratio of the evanescent field power in the cladding to the total power of the waveguide mode. Huang et al. calculated the EFR which exceeds 25% for silicon on sapphire slot waveguides in the mid-IR region for the detection of CO_2 gas (*14*). Ranacher et al. has developed a spectroscopic gas sensor by utilizing EFR (*15*). Kumari et al. proposed a mid-IR evanescent gas sensor based on silicon-on-nitride slot waveguide obtaining an evanescent field fraction of 43% (*16*). The sensors with high EFR can interact more with the absorbing medium, which in turn improves the sensitivity of the sensor. However, there is a drawback of a higher EFR: the mode is less confined in the waveguide, which leads to a higher spurious damping and leakage of the mode. The geometrical dependence of EFR, as well as propagation loss, provides a guideline for the design of optical waveguide for mid-IR absorption sensing application. For sensing purposes, the optical waveguide structure has to be designed to assure a high sensitivity, that is, the sensor response for changes in the optical properties of the cover medium has to be as high as possible. This sensitivity depends on the strength and distribution of the evanescent field in the outer medium. The existence of a species may be sensed by its direct influence on the evanescent field of an optical wave travelling in the waveguide.

Waveguide design and EFR calculation

In this work, silicon on silicon dioxide (Si/SiO_2) strip waveguides is modelled using commercial finite element method (FEM) simulation tool COMSOL multiphysics 5.1. The structures were designed for a wavelength of 3.39 μm, which corresponds to an absorption line of CH_4 in mid-IR. Generally, a waveguide with the small electrical field is desired to support a strong evanescent field (*17*). The EFR values are optimized depending on the geometry of the waveguide. The schematic of a strip waveguide is shown in Figure 2(a), where H and W are the height and width of the strip waveguide, respectively. In strip waveguide, both quasi-TE and quasi-TM modes are studied, because of the likely gas interaction with the evanescent field on the top and at the sidewalls of the waveguide. For quasi-TE mode, the dominant electrical field is in the horizontal direction. The electrical field jumps up because it has a lower dielectric constant in the gas as compared to a dielectric constant in silicon core as shown in Figure 2(b).

In Figure 2(b), it can be seen that the evanescent field is quite strong. Therefore, the waveguide dimensions are optimized to obtain the maximum EFR without creating a leaky quasi-TE mode. As the waveguide dimensions are reduced, the mode gets squeezed and the evanescent field can jump to even higher level. This, in turn, leads to an

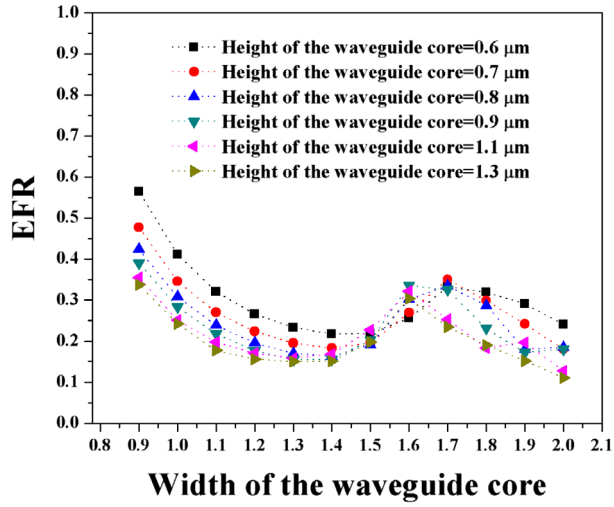

Figure 3. Quasi-TE mode in a strip waveguide, EFR vs. waveguide width.

increase in the EFR as shown in Figure 3. Though, there is a limit on narrowing the dimensions of the waveguide. When W gets too small ($W < 0.9$ μm) the quasi-TE mode gets leaky and it is no longer supported as a guiding mode and all the energy is transferred to the cladding. EFR saturates for large W values ($W > 2$ μm) because most of the energy is confined laterally in the silicon core and most of the evanescent field will be from the top wall interface. Moreover, in the vertical direction, EFR doesn't depend so much on the waveguide height H, but shrinkage of H can still enhance the EFR value as can be seen in Figure 3.

In the case of quasi-TM mode propagation in a waveguide, the vertical electrical field is dominant. This is for the same reason as in the quasi-TE mode, the evanescent field is enhanced at the top cladding as shown in Figure 4(a). The EFR is sensitive to waveguide height and it depends on H in a similar fashion as it does on W in the quasi-TE mode as shown in Figure 4(b). Meanwhile, larger waveguide width affects the EFR value. Waveguide becomes leaky when W and H become too small.

Total propagation loss of the waveguide

Moreover, we also considered the total losses of the waveguide. The total propagation losses of the strip waveguide were calculated using the expression as shown in Figure 5(a). The input and output powers were calculated by integrating the power in the input and output surfaces of the waveguide. Strip waveguide shows a loss of 2.12–3.16 dB and 1.91–2.14 dB for quasi-TM and quasi-TE modes, respectively. The loss in the quasi-TE mode is lower than that in the quasi-TM mode for slightly different waveguide dimensions. This is possibly due to the enhancement of electrical field at the side walls as shown in Figures 2(b) and 4(a). Increasing

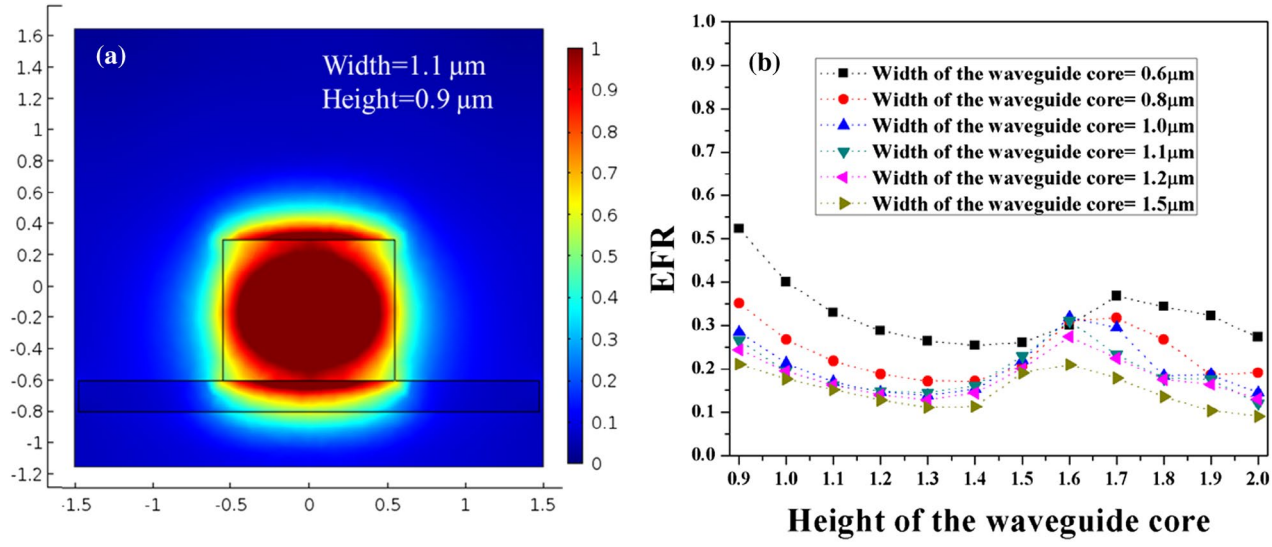

Figure 4. Quasi-TM mode in a strip waveguide (a) Mode distribution at 3.39 microns (W = 1.1 microns, H = 0.9 microns) and (b) EFR vs. waveguide height.

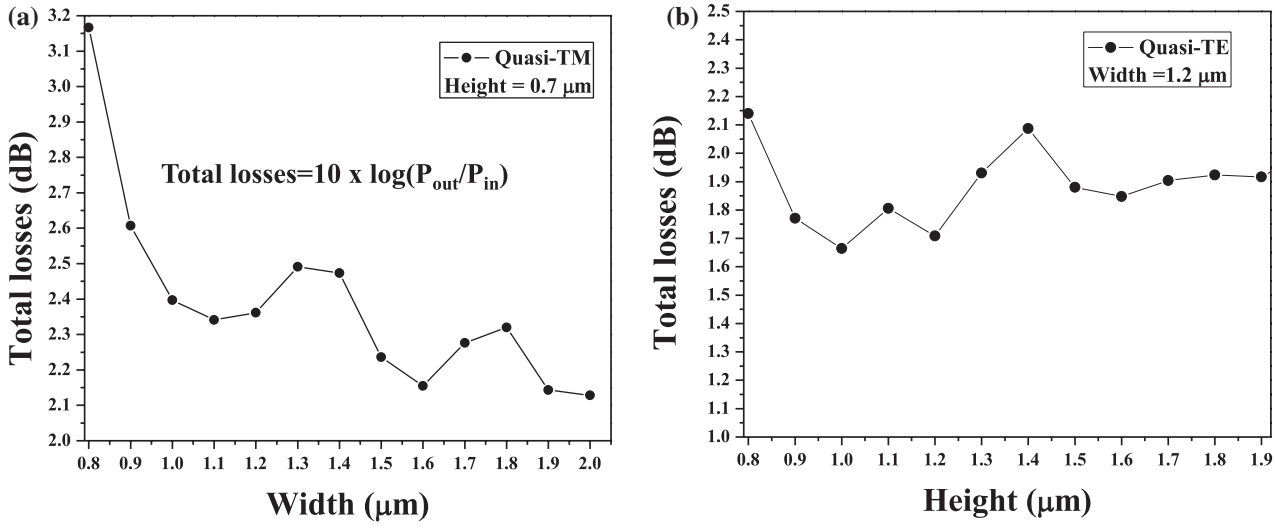

Figure 5. Total propagation loss for strip waveguide of length 5 μm, (a) Quasi-TM polarization and (b) quasi-TE polarization.

the width (for TM polarization) and height (for TE polarization) of a waveguide reduces the propagation loss by weakening the electrical field at the two sidewalls for both TM (Figure 5(a)) and TE (Figure 5(b)) modes.

Dependence of EFR and sensitivity of the gas sensor on the waveguide length

The EFR highly depends on the waveguide dimensions. Smaller waveguide dimensions have high EFR as can be seen from Figures 3 and 4(b). The EFR dependence on the total length of the waveguide was studied using the parametric sweep function of COMSOL. Even though, the high aspect ratio of the strip waveguide, the FEM simulations were carried out in three-dimensional models which were a bit lengthy and time-consuming process. The dimensions of the waveguides were fixed to certain values and the EFR was calculated for every propagation length with a step size of 1 μm. As it can be seen from the Figure 6, the EFR decreases with the increasing length of the waveguide due to the fact that propagation losses are directly related to the increase of the waveguide length.

On the other hand, sensitivity is directly related to the optimal length of the waveguide sensor as expressed in Equation (1).

$$S = -\eta\varepsilon l I_0 \exp(-\eta\varepsilon c l - \alpha_0 l) \tag{1}$$

where S is the sensitivity of the gas sensor, I_0 is the input power; ε and c are the absorption coefficient and the

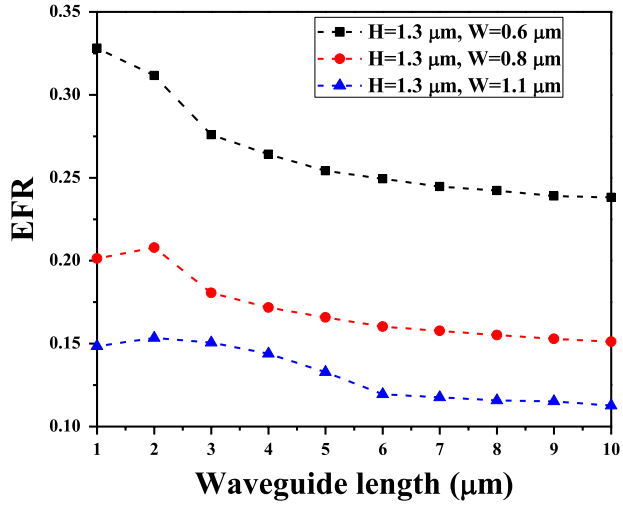

Figure 6. EFR value dependence on the propagation of length of a waveguide.

concentration of the target gas, respectively; l is the length of the waveguide and α_0 is the total losses of the waveguide and η is the EFR value at a specific length. For example, CH_4 has an absorption coefficient $\varepsilon = 8.2 \times 10^{-5}$ Pa^{-1} cm^{-1} (8.3 atm^{-1} cm^{-1}) for 3.392 μm line of a He–Ne laser (*18*). The combination and overtone absorption bands of methane at 1.33 and 1.66 μm have much weaker absorption coefficients. The increase in the sensitivity of the gas sensor is a result of longer interaction path. When the path length gets longer than the optimal value, however, the sensitivity begins to drop due to the over-attenuation of the signal, which can be alleviated by lowering the intrinsic loss.

Conclusion

Silicon strip waveguide designs are optimized to develop an evanescent field absorption gas sensor for methane for quasi-TE and quasi-TM at 3.39 μm. These waveguides can provide an EFR of greater than 55% with moderate waveguide dimensions. The total propagation losses of these waveguides were also calculated which are in the range of 2–3 dB for quasi-TE and quasi-TM modes, respectively. EFR and sensitivity of the evanescent absorption sensor are highly dependent on the propagation length of the waveguide. Moreover, these waveguides can deliver a wide-ranging platform for adaptable sensing of diverse types of gases in a reusable manner by changing the fundamental wavelength corresponds to the absorption line for an extensive variety of trace gases.

Disclosure statement

No potential conflict of interest was reported by the authors.

Funding

This work was supported by the Ministry of Education and Science of the Russian Federation and the Russian Foundation for Basic Research [grant number 16-29-11698, 16-29-11744].

ORCID

M. A. Butt http://orcid.org/0000-0003-0829-4886

References

(1) Kohl, D. Function and Applications of Gas Sensors. *J. Phys. D: Appl. Phys.* **2001**, *34*, R125–R149. DOI: 10.1088/0022-3727/34/19/201.

(2) Arshak, K.; Moore, E.; Lyons, G.M.; Harris, J.; Clifford, S. A Review of Gas Sensors Employed in Electronic Nose Applications. *Sens. Rev.* **2004**, *24*, 181–198. DOI: 10.1108/02602280410525977.

(3) Huang, Y.; Kalyoncu, S.; Song, Q.; Boyraz, O. *Silicon-on-Sapphire Waveguides Design for mid-IR Evanescent Field Absorption Gas Sensors*. Conference on Lasers and Electro-optics, Optical Society of America: San Jose, CA, **2012**; JW2A.122. DOI: 10.1364/CLEO_AT.2012.JW2A.122.

(4) Micheal, B.F.; Raji, S.; Irfan, B.; Ian, F.; Mathew, C.L.; Richard T.W.; Mark, G.A.; Marko, L. Progress toward mid-IR chip-scale integrated-optic TDLAS gas sensors. Quantum Sensing and Nanophotonic Devices X, **2013**; 86310E. DOI: 10.1117/12.2008953.

(5) Stewart, G.; Jin, W.; Culshaw, B. Prospects for Fibre-optic Evanescent-field Gas Sensors Using Absorption in the near-Infrared. *Sens. Actuators B*. **1997**, *38*, 42–47. DOI: 10.1016/S0925-4005(97)80169-4.

(6) Siebert, R.; Müller, J. Infrared Integrated Optical Evanescent Field Sensor for Gas Analysis Part I: System Design, *Sens. Actuators A*. **2005**, *119*, 138–149. DOI: 10.1016/j.sna.2004.11.001.

(7) Degtyarev, S.A.; Butt, M.A.; Khonina, S.N.; Skidanov, R.V. *Modelling of TiO_2 Based Slot Waveguides with High Optical Confinement in Sharp Bends*. International Conference on Computing, Electronic and Electrical Engineering, **2016**; pp 10–13. DOI: 10.1109/ICECUBE.2016.7495222.

(8) Butt, M.A.; Sole, R.; Pujol, M.C.; Rodenas, A.; Lifante, G.; Choudhary, A.; Murugan, G.S.; Shepherd, D.P.; Wilkinson, J.S.; Aguilo, M.; Diaz, F. Fabrication of Y-Splitters and Mach–Zehnder Structures on (Yb,Nb):$RbTiOPO_4$/$RbTiOPO_4$ Epitaxial Layers by Reactive Ion Etching. *J. Lightwave Technol.* **2015**, *33*, 1863–1871. DOI: 10.1109/JLT.2014.2379091.

(9) Butt, M.A.; Pujol, M.C.; Sole, R.; Rodenas, A.; Lifante, G.; Aguilo, M.; Diaz, F.; Khonina, S.N.; Skidanov, R.V.; Verma, P. *Fabrication of Optical Waveguides in $RbTiOPO_4$ Single Crystals by Using Different Techniques*, 14th International Conference on Optical Technologies for Telecommunications, Ufa, Russian Federation, **2015**; 98070C. DOI: 10.1117/12.2231368.

(10) Butt, M.A.; Kozlova, E.S.; Khonina, S.N.; Skidanov, R.V. *Optical Planar Waveguide Sensor Based on (Yb,Nb): RTP/RTP (0 0 1) System for the Estimation of Metal Coated Cells*, International Conference Information Technology

and Nanotechnology, Samara, Russia, **2016**; pp 16–23. DOI: 10.18287/1613-0073-2016-1638-16-23.

(11) Butt, M.A.; Kozlova, E.S.; Khonina, S.N.; Skidanov, R.V. *Modelling of the Optical Planar Waveguide Based on (Yb,Nb):RTP(0 0 1) System for Cell Counting*, 1st International Conference on Computing, Electronic and Electrical Engineering, Delhi, India, **2016**; pp 63–67. DOI: 10.1109/ICECUBE.2016.7495256.

(12) Ian, J.D. Does Methane Pose Significant Health and Public Safety Hazards? A Review. *Environ. Geosci.* **2015**, *22*, 85–96.

(13) Prasad S.; Zhao L.; Gomes J. *Methane and Natural Gas Exposure Limits*, ISEE 22nd Annual Conference, **2010**; p S251. DOI: 10.1097/01.ede.0000392463.93990.1e.

(14) Huang, Y.; Kalyoncu, S.K.; Zhao, Q.; Torun, R.; Boyraz, O. Silicon on Sapphire Waveguides Design for the Mid IR Evanescent Field Absorption Gas Sensors, *Opt. Commun.* **2014**, *313*, 186–194.DOI:

(15) Ranacher, C.; Consani, C.; Maier, F.J.; Hedenig, U.; Jannesari, R.; Lavchiev, V.; Tortschanoff, A.; Grille, T.; Jakoby, B. *Spectroscopic Gas Sensing Using a Silicon Slab Waveguide*, 30th Eurosensors Conference, EUROSENSORS, Budapest, Hungary, **2016**: *168*, pp 1265–1269. DOI: 10.1016/j.proeng.2016.11.444.

(16) Kumari, B.; Barh, A.; Varshney, R.K.; Pal, B.P. *Mid-IR Evanescent Field Gas Sensor Based on Silicon-on-Nitride Slot Waveguide*, 12th International Conference on Fiber Optics and Photonics, Kharagpur, India, **2014**. DOI: 10.1364/Photonics.2014.M4A.12.

(17) Densmore, A.; Xu, D.X.; Waldron, P.; Janz, S.; Cheben, P.; Lapointe, J.; Delge, A. A Silicon-on-Insulator Photonic Wire Based Evanescent Field Sensor, *IEEE Photonics Technol. Lett.* **2006**, *18*, 2520–2522. DOI:

(18) Tai, H.; Tanaka, H.; Yoshino, T. Fibre-optic Evanescent-Wave Methane Gas Sensor Using Optical Absorption for the 3.392 μm Line of a He–Ne Laser, *Opt. Lett.* **1987**, *12*, 437–439.DOI: